Direct pressure sensing with carbon nanotubes grown in a micro-cavity

A. S. Chauhan and A. Nogaret[a)]
Department of Physics, University of Bath, Bath BA2 7AY, United Kingdom

(Received 30 October 2012; accepted 31 May 2013; published online 12 June 2013)

We report on the growth of multiwall carbon nanotubes (CNTs) at the centre of a bow tie micro-cavity and describe the change in resistance of these CNTs under gas pressure loading ($\Delta R/R \cong 16\%$/atm). By adapting the Euler-Bernoulli theory of beams to CNTs that bridge opposite walls of the cavity, we fit the piezoresistance curves and extract the Young's modulus, the piezoresistive constant, and the nanotube radius, for a range of CNT growth conditions. By detecting pressures as low as 0.1 atm, we demonstrate a membrane-less technology capable of sensing pressure with micron scale resolution. © *2013 AIP Publishing LLC*. [http://dx.doi.org/10.1063/1.4811166]

The electromechanical properties of carbon nanotubes (CNTs) are the focus of intense interest both in experiments that use strain as a tool[1–8] for investigating the electronic structure of CNTs and in devices that use the piezoresistance of CNTs for sensing pressure.[9–12] Cao *et al.*[13] have reported the highest piezoresistance to date in quasi-metallic single wall CNTs by measuring a strain gauge factor 5 times larger than either polysilicon[14] or GaAs.[15] The piezoresistance of multiwall CNTs is known to arise from the telescopic sliding of CNT shells[6] which increases the CNT resistance when CNTs are subjected to either tensile[16] or compressive[17] strain. Both CNT[11,12] and GaAs (Ref. 15) strain transducers have been fabricated on micro-machined membranes for sensing pressure. These membranes remain difficult to scale down below a few hundred microns because a minimum amount of drum deformation is necessary to warrant sufficient pressure sensitivity. Recent proposals for taming turbulence[18] call for even smaller pressure sensors to visualize vortex nucleation to within 26 μm, a resolution inaccessible with current devices.

Here, we report on the direct detection of gas pressure by CNTs grown inside micro-machined silicon cavities with cross-section as small as 2 μm^2. The CNTs behave as nano-sails anchored to both ends whose resistance increases with gas pressure. This differs from earlier studies where strain was applied by Atomic Force Microscope tips[6–9] or moving parts[10–13] for which a strain gauge factor could be defined. Our CNTs were grown by chemical vapour deposition (CVD) of CH_4 until they anchor themselves to the opposite walls of the cavity. We monitor this process by measuring the wall-to-wall resistance during CVD growth. We study the piezoresistance of CNTs prepared under different growth conditions: temperature, time, and methane flow rate. The piezoresistance is found to be as high as 16% at 1 atm compared to 3.5%/atm for GaAs membranes.[15] We show that the change in resistance with pressure is well described by Euler-Bernoulli theory modeling CNTs as elastic beams which are free to pivot at anchor points. A fit of the experimental piezoresistance curves with this theory obtains the Young modulus of CNTs, the piezoresistive constant, and the average radius of the CNTs which we find to be in good agreement with either the published values or the CNT dimensions on electron microscope images.

The cavities were micro-machined from n-doped Si(100) wafer (resistivity: 0.3 Ω cm) capped with 30 nm of native oxide. Two $4 \times 4\,mm^2$ wafer slabs were cleaved and processed as the *top* and *bottom elements* of the cavity. These slabs form the electrodes between which the resistance of the CNTs is measured (Figure 1(a)). Additional SiO_2 was deposited on the bottom slab by dual ion beam sputtering to increase the thickness of the original layer to 250 nm and electrically insulate the top electrode from the bottom electrode. The bottom slab was then etched in the form of a bow tie constriction using optical lithography and reactive ion etching (CHF_3/SF_6). Two types of constrictions were produced with widths of 2 μm and 20 μm and heights of 1 μm and 2.3 μm, respectively. The constriction forms the active region of the micro-cavity: a region of maximum pressure gradient where CNTs are grown (Figure 1(a)). A thin Ni film (3 nm) was then deposited over the constriction to catalyse the growth of CNTs. Thermal evaporation and lift-off techniques were used to deposit Ni over an area of 50 μm × 50 μm centred on the constriction. The Ni film was evaporated over the top slab after its SiO_2 layer had been stripped off by hydrofluoric acid etch. 150 nm thick Au contacts were then fabricated on the back surfaces of the top and bottom slabs. The top slab was flipped over the bottom slab to form the micro-cavity (Figures 1(b) and 1(c)). The two slabs were sealed together using sodium silicate (Na_2SiO_3:H_2O) cured at 750 °C. Curing also allowed the Ni film to coalesce into 25–40 nm Ni islands which catalysed the growth of CNTs. Following CNT growth, electrical wires were attached with silver-epoxy to the Au contacts. The device was inserted in a sealed enclosure (Figure 1(d)) to measure the change of resistance of the cavity as a function of the gas pressure applied to it.

CNT growth began by flushing the CVD chamber with H_2 gas (flow rate: 400 sccm) for 15 min prior to the admission of CH_4 (40 sccm or 60 sccm). CH_4 molecules decompose on the Ni islands which catalyse the assembly of the carbon network and seed the growth of CNTs. To determine the time it takes for CNTs, to bridge the cavity and contact the opposite wall, we monitor the resistance of the cavity *in-situ* during growth, using a pair of metal clamps that connect the top and bottom slabs to electrical measurement

a)Email: A.R.Nogaret@bath.ac.uk. Tel: +44 (0)1225 385609.

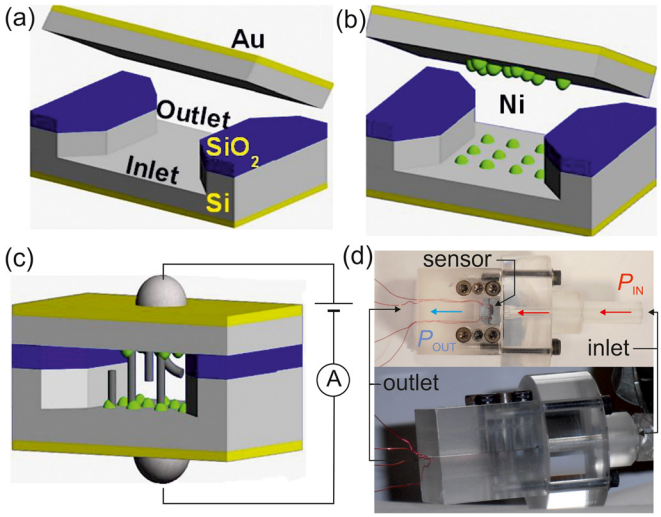

FIG. 1. Bow tie pressure sensor: (a) a bow tie constriction 2 μm-20 μm wide is plasma etched in a Si/SiO_2 wafer; (b) islands of Ni catalyst are fabricated at its centre; (c) the top and bottom slabs are sealed together before the CNTs are grown by CVD of methane; (d) the bow tie pressure sensor is inserted in a sealed enclosure that allows the resistance of the CNTs to be monitored as a function of the pressure difference $\Delta P = P_{IN} - P_{OUT}$ between inlet and outlet. Slab surface area: 4 mm × 4 mm.

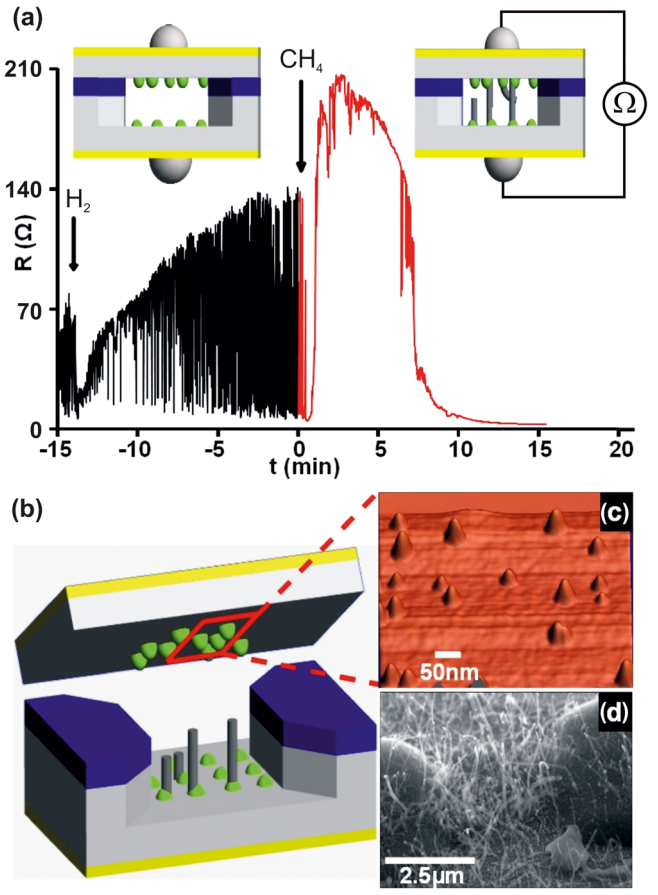

FIG. 2. (a) Resistance of CNTs monitored *in situ* during CVD growth at 875 °C. CNTs start bridging the 2.3 μm tall cavity 6 min after the admission of methane; (b) CNTs in cavity; (c) AFM image of Ni islands (catalyst); (d) SEM micrograph of CNTs grown in a 2 μm wide constriction (with top slab removed).

apparatus outside the CVD chamber. The time dependence of the cavity resistance is shown in Figure 2(a). The resistance starts dropping 6 min after the admission of CH_4 which signals the onset of conduction through CNTs (Figures 2(b)–2(d)). The accepted CNT growth rate[19,20] (1200 nm/min) suggests that CNTs bridge the 2.3 μm gap in 2 min. The 4 extra minutes prior to the resistance drop may be required for CNT endings to migrate on the opposite surface until they attach to a Ni island. Another possibility is that the diffusion rate of methane is lower in the confined space of the cavity. We have grown CNTs over 8, 9, 10, 11, and 12 min, in methane flow rates of 40 sccm and 60 sccm and at temperatures of 800 °C, 850 °C, 875 °C, and 900 °C to obtain various CNT densities and CNT radii. SEM micrographs show that CNTs tend to grow with random orientations (Figure 2(d)).

The growth temperature is the main parameter controlling CNT growth. At temperatures below 850 °C, CNT grow sparsely (Figure 3(a)). This is confirmed by X-ray energy dispersive spectra (X-EDS) that show residual traces of carbon in the cavity at 800 °C and 850 °C (Figure 3(a)). The concentration of CNTs increases dramatically once growth temperature reaches 875 °C. The CNT radius is $a \approx 12$ nm at 800 °C-875 °C, rising to $a \approx 25$ nm at 900 °C. Now turning to the I-V curves measured across the cavity (Figure 3(b)), CNTs grown at 875 °C and 900 °C are *quasi metallic*. Their I-V curves remain Ohmic down to 77 K (Figure 3(c)). The current follows a thermionic activation law[21] characterized by a work function of 12 meV. This behavior is consistent with multi-wall CNTs incorporating structural defects. The resistance of the device prepared at 875 °C corresponds to 10–12 CNTs bridging the cavity. In contrast, CNTs grown at lower temperature (800 °C, 850 °C) are *semiconductors*. Figure 3(c) shows that their zero bias conductance vanishes at 77 K. We have verified that CNTs require anchoring to Ni islands on opposite walls of the cavity in order to conduct. CNTs grown in a cavity having Ni islands on one wall only led to an increase in cavity resistance by a factor of 10^5. Furthermore, X-EDS spectra taken in the Si and SiO_2 areas of slabs revealed no carbon residues susceptible of giving current leakage.

Next, we inserted the sensor in the hermetically sealed enclosure of Figure 1(d) to monitor the resistance of the cavity as a function of the pressure of N_2 gas applied across it. The CNTs remained in N_2 atmosphere throughout to avoid changes in resistance induced by oxidation.[22] We focused on cavities with multiwall CNTs grown at 875 °C. Pressure is found to increase the cavity resistance (Figure 4) as multiwall CNTs are put under tensile strain.[6,11,13,16] Initially, the piezoresistance $\Delta R/R$ increases quadratically then saturates.

To explain the pressure response, we construct a theory assimilating CNTs to elastic nano-beams characterized by their Young's modulus E and length L. We further assume that the modelled CNTs grow perpendicular to the top and bottom slabs (x-axis) and that the anchor points apply no bending moment to their extremities. The piezoresistance is given by

$$\frac{\Delta R}{R} = \pi_L E \frac{\Delta L}{L}, \quad (1)$$

where π_L is the piezoresistive constant and $\Delta L/L$ is the axial strain due to gas pressure $\Delta P = P_{IN} - P_{OUT}$. The force applied per unit length of the nanotube is $q = 2a\Delta P$, where a is the

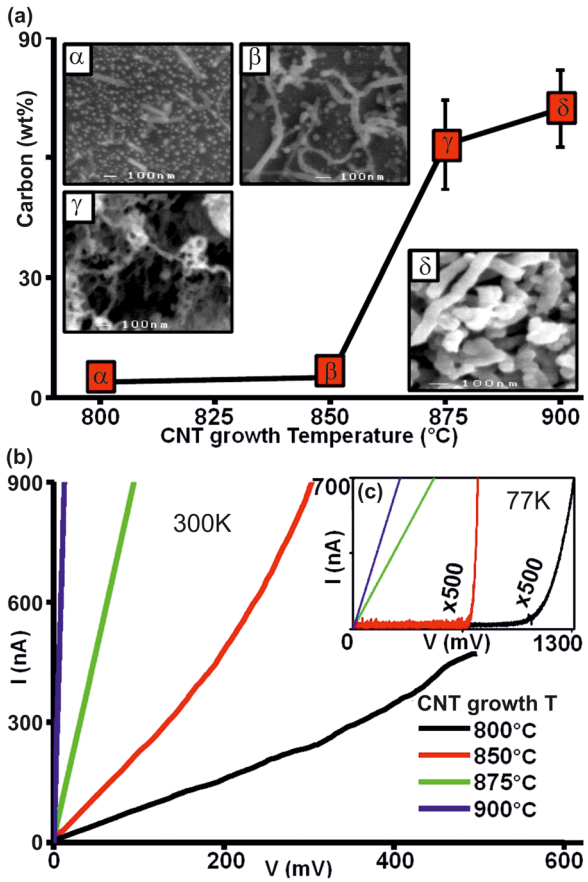

FIG. 3. (a) Carbon concentration (X-EDS) in the bow tie at different growth temperatures: (α) 800 °C, (β) 850 °C, (γ) 875 °C, and (δ) 900 °C; (b) and (c) I–V curves of the corresponding CNTs measured at (b) 300 K and (c) 77 K.

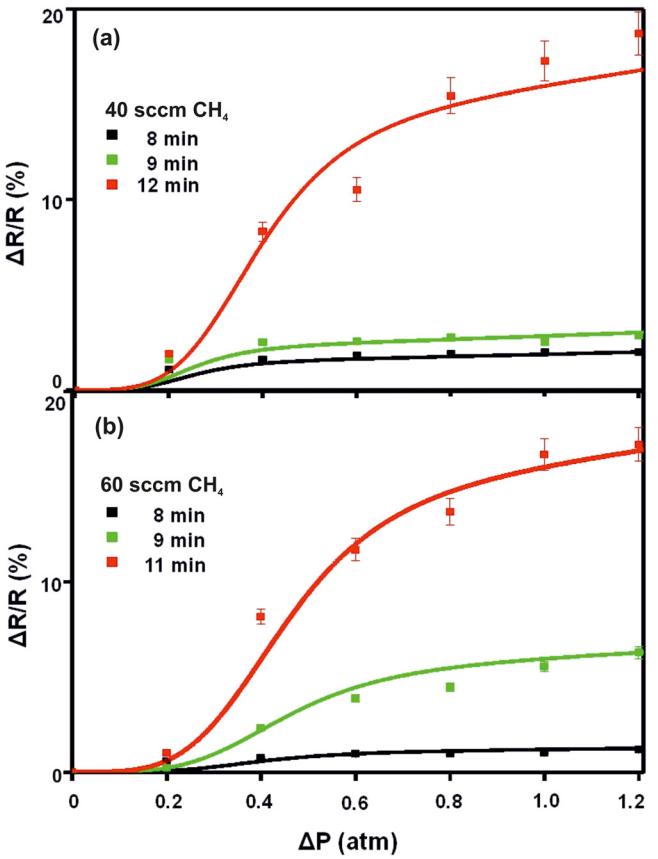

FIG. 4. Variation in CNT resistance as a function of the N_2 pressure applied across the bow tie constriction. CNTs were grown at 875 °C. The symbols show the piezoresistance of CNTs grown under different methane flow rates: (a) 40 sccm and (b) 60 sccm for growth times varying between 8 min and 12 min. These data are fitted with Eq. (8) (full lines). $L = 1\,\mu$m.

CNT radius. We compute the axial strain by solving the Euler-Bernoulli equation

$$\frac{d^2M}{dx^2} + \frac{T_x}{EI}M = -q, \tag{2}$$

using $M(\pm L/2) = 0$ for the boundary conditions on the bending moment at each end of the CNT. $I = \pi a^4/4$ is the second moment of inertia of the nanotube and T_x is the tension normal to the interface at anchor points. The bending moment relates to the transverse deflection of the beam $y(x)$ through

$$M = -EI\frac{d^2y}{dx^2}. \tag{3}$$

Integrating Eqs. (2) and (3) with boundary conditions $y(\pm L/2) = 0$ gives the slope of the beam

$$\frac{dy}{dx} = -\frac{q}{T_x}\left[\frac{1}{k}\frac{\sin(kx)}{\cos(kL/2)} - x\right], \tag{4}$$

where $k = \sqrt{T_x/EI}$ is the deformation wavevector. The strain in the CNT then follows as

$$\frac{\Delta L}{L} = \frac{1}{L}\int_{-L/2}^{+L/2} dx\left(\sqrt{1+\left(\frac{dy}{dx}\right)^2} - 1\right). \tag{5}$$

Inserting Eq. (5) into Eq. (1) gives the piezoresistance which is the equation we seek to model the pressure dependence in Figure 4. In Eq. (4) however, T_x implicitly depends on q. This dependency is made explicit by writing the stress-strain relation $T = E\pi a^2\Delta L/L$, where T is the tension in the CNT. T relates to its axial vector component T_x through $T_x = T\left[1+\left(\frac{dy}{dx}\right)^2_{L/2}\right]^{-1/2}$, which one expands as

$$T_x = \frac{E\pi a^2}{L}\int_{-L/2}^{+L/2} dx\frac{\sqrt{1+\left(\frac{dy}{dx}\right)^2} - 1}{\sqrt{1+\left(\frac{dy}{dx}\right)^2_{L/2}}}. \tag{6}$$

For small deflections of the beam $dy \ll dx$, Eq. (6) writes to second order as

$$T_x = \frac{EI}{L^2}x_p^2 = \frac{EI}{L^2}\frac{\frac{34}{315\pi^2}\left(\frac{\Delta P}{E}\right)^2\rho^8}{1+\frac{1}{18\pi^2}\left(\frac{\Delta P}{E}\right)^2\rho^6}, \tag{7}$$

where $\rho = L/a$. Equation (7) was next inserted into Eqs. (4), (5), and (1) to obtain the theoretical piezoresistance. This calculation is the first which considers the present boundary conditions and describes the change of tension with strain. The leading terms in the piezoresistance are

TABLE I. Young's moduli (E), piezoresistive constants (π_L), and CNT radii (a) obtained by fitting Eq. (8) to the piezoresistance data of Fig. 4.

	40 sccm CH_3			60 sccm CH_3		
t (mn)	E (TPa)	π_L (TPa^{-1})	a (nm)	E (TPa)	π_L (TPa^{-1})	a (nm)
8	0.17	14	11	0.13	13	12.5
9	0.20	18	11	0.35	28	13
10	0.24	20	12	0.40	45	13
11	…	…	…	0.47	50	13
12	0.47	48	12.5	…	…	…

$$\frac{\Delta R}{R} = \pi_L E\left\{\left(\frac{17}{630\pi^2} + \frac{31}{5670\pi^2}x_p^2\right)\left(\frac{\Delta P}{E}\right)^2 \rho^6 - \frac{1801}{3243240\pi^4}\left(\frac{\Delta P}{E}\right)^4 \rho^{12} + O(\Delta P^6)\right\}. \quad (8)$$

The quadratic dependence is a consequence of the elongation of the beam. This elongation is independent of the direction in which pressure is applied, hence the symmetry with respect to a change in sign of ΔP. At higher pressure, deformation of the CNT means that pressure loading becomes uneven across its length. The saturation of the piezoresistance occurs when loading increases at the centre of the CNT relative to its ends. We used Eq. (8) to fit the data in Fig. 4 and obtain π_L, E, and a as adjustment parameters (using $L = 1\ \mu$m in $\rho = L/a$). The data are summarized in Table I.

We find that E and π_L increase with growth time increasing the device sensitivity as shown in Figure 4 and Table I. Young's moduli of 0.13-0.47 TPa are lower than the 1 TPa expected from pristine single wall CNTs[23–25] but are in good agreement with the values expected from multi-wall CNTs.[26–28] The thermo-mechanical annealing of Stone-Wale structural defects[29] and the migration of vacancies and adatoms[30] is likely to explain the increase in Young's modulus when the growth time increases from 8 min to 12 min. The fit of the piezoresistance data in Figure 4 further yields the radii of CNTs, which are in excellent agreement with radii measured from scanning and transmission electron micrographs (Figure 3(a)). These results validate the assumptions made when building the theory.

In summary, we have grown carbon nanotubes inside a silicon micro-cavity and have evidenced a temperature threshold above which CNTs self-anchor to opposite sides of the cavity and conduct. By applying gas pressure to the cavity, the embedded nanotubes bend causing the resistance to change as predicted by the Euler-Bernoulli theory. Fitting the theory to the experimental data accurately estimates the radius of CNTs, their Young modulus, and piezoresistive constant. The proposed pressure sensor was scaled to a cross-sectional area of 2 μm^2, which is four orders of magnitude smaller than current membrane sensors.

[1]T. W. Odom, J.-L. Huang, P. Kim, and C. M. Lieber, Nature **391**, 62–64 (1998).
[2]A. Bachtold, M. S. Fuhrer, S. Plyasunov, M. Forero, E. H. Anderson, A. Zettl, and P. L. McEuen, Phys. Rev. Lett. **84**, 6082 (2000).
[3]R. Heyd, A. Charlier, and E. McRae, Phys. Rev. B **55**, 6820 (1997).
[4]A. Maiti, A. Svizhenko, and M. P. Anantram, Phys. Rev. Lett. **88**, 126805 (2002).
[5]L. Yang and J. Han, Phys. Rev. Lett. **85**, 154 (2000).
[6]J. Cumings and A. Zettl, Phys. Rev. Lett. **93**, 086801 (2004).
[7]T. Kuzumaki and Y. Mitsuda, Appl. Phys. Lett. **85**, 1250 (2004).
[8]V. Semet, V. Thien Binh, D. Guillot, K. B. K. Teo, M. Chhowalla, G. A. J. Amaratunga, W. I. Milne, P. Legagneux, and D. Pribat, Appl. Phys. Lett. **87**, 223103 (2005).
[9]R. J. Grow, Q. Wang, J. Cao, D. Wang, and H. Dai, Appl. Phys. Lett. **86**, 093104 (2005).
[10]C. Hierold, A. Jungen, C. Stampfer, and T. Helbling, Sens. Actuators, A **136**, 51–61 (2007).
[11]C. Stampfer, T. Helbling, D. Obergfell, B. Schöberle, M. K. Tripp, A. Jungen, S. Roth, V. M. Bright, and C. Hierold, Nano Lett. **6**, 233–237 (2006).
[12]A. A. Farajian, B. I. Yakobson, H. Mizuseki, and Y. Kawazoe, Phys. Rev. B **67**, 205423 (2003).
[13]J. Cao, Q. Wang, and H. Dai, Phys. Rev. Lett. **90**, 157601 (2003).
[14]P. J. French and A. G. R. Evans, Solid State Electron. **32**, 1–10 (1989).
[15]A. Dehé, K. Fricke, K. Mutamba, and H. L. Hartnagel, J. Micromech. Microeng. **5**, 139–142 (1995).
[16]T. W. Tombler, C. Zhou, L. Alexeyev, J. Kong, H. Dai, L. Liu, C. S. Jayanti, M. Tang, and S.-Y. Wu, Nature **405**, 769 (2000).
[17]Z.-M. Dang, M.-J. Jiang, D. Xie, S.-H. Yao, L.-Q. Zang, and J. Bai, J. Appl. Phys. **104**, 024114 (2008).
[18]M. Gad-El-Hak, Act. Flow Control **95**, 1–24 (2007).
[19]R. Rao, D. Liptak, T. Cherukuri, B. I. Yakobson, and B. Maruyama, Nature Mater. **11**, 213 (2012).
[20]M. A. Ribas, F. Ding, P. B. Balbuena, and B. I. Yakobson, J. Chem. Phys. **131**, 224501 (2009).
[21]O. W. Richardson, Science **38**, 57–61 (1913).
[22]C. S. Huang, B. R. Huang, Y. H. Jang, M. S. Tsai, and C. Y. Yeh, Diamond Relat. Mater. **14**, 1872 (2005).
[23]M. M. J. Treacy, T. W. Ebbesen, and J. M. Gibson, Nature **381**, 678 (1996).
[24]A. Krishnan, E. Dujardin, and T. W. Ebbesen, Phys. Rev. B **58**, 14013 (1998).
[25]E. W. Wong, P. E. Sheehan, and C. M. Lieber, Science **277**, 1971 (1997).
[26]M.-F. Yu, O. Lourie, M. J. Dyer, K. Moloni, T. F. Kelly, and R. S. Ruoff, Science **287**, 637 (2000).
[27]J.-P. Salvetat, A. J. Kulik, J.-M. Bonard, G. A. D. Briggs, T. Stöckli, K. Méténier, S. Bonnamy, F. Béguin, N. A. Burnham, and L. Forró, Adv. Mater. **11**, 161 (1999).
[28]X.-L. Wei, Y. Liu, Q. Chen, M.-S. Wang, and L.-M. Peng, Adv. Funct. Mater. **18**, 1555 (2008).
[29]C. Shet, N. Chandra, and S. Namilae, J. Mater. Sci. **40**, 27–36 (2005).
[30]F. Banhart, J. Kotakoski, and A. V. Krasheninnikov, ACS Nano **5**, 26 (2011).